IEEE Access
Multidisciplinary | Rapid Review | Open Access Journal

Received 14 February 2024, accepted 17 April 2024, date of publication 1 May 2024, date of current version 13 May 2024.

Digital Object Identifier 10.1109/ACCESS.2024.3396066

RESEARCH ARTICLE

Single Spring Gravity Compensator for a Multi-DOF Manipulator

KRITTANAI SAJJAPONGSE AND WITAYA WANNASUPHOPRASIT
Mechanical Engineering Department, Chulalongkorn University, Bangkok 10330, Thailand

Corresponding author: Witaya Wannasuphoprasit (witaya.w@chula.ac.th)

This work was supported in part by the Graduate School, Chulalongkorn University; and in part by the Mechanical Engineering Department.

ABSTRACT Robotic manipulators are typically engineered with high-power systems to handle payloads and counteract gravity, owing to their robust and weighty structures. However, there is now a growing need for eco-friendly and safe human-robot collaboration solutions that require power-efficient innovations. Currently, gravity compensation techniques employ various counterbalancing mechanisms that are specific and challenging to expand for systems with higher degrees of freedom (DOF). In response, this research introduces a novel gravity compensator system capable of effectively counterbalancing manipulators with multiple degrees of freedom (DOF) using only one spring. The proposed system uses parallelogram mechanisms, cam follower systems, and a square-root mechanism to solve potential equations mechanically. The proposed system can generalize the design of a gravity compensator for a multi-DOF manipulator using only one linear spring. This paper outlines the design and development of prototypes, focusing on one- and three-degree-of-freedom manipulators, which serve as experimental testbeds. The experiment shows that our gravity compensator system significantly reduces the required torques, power, and overall energy consumption of the robotic system. This innovative approach addresses existing challenges and paves the way for sustainable and power-efficient robotic manipulator design.

INDEX TERMS Gravity compensator, low power, manipulator, robotic arm, multi DOF.

I. INTRODUCTION

Manipulator arms are widely used in various industries including manufacturing, healthcare, entertainment, and services. However, owing to their high-power actuators, these robotic arms can pose safety risks to operators and the working environment because they are heavy and have significant inertia. To mitigate this issue, gravity compensators, such as counterweights or spring mechanisms, are employed to reduce the load of actuators in the manipulator arms.

It is worth noting that as the manipulator arm operates, the center of gravity changes continuously, making the design of multi-DOF (degree of freedom) gravity compensators challenging. This research focuses on passive gravity compensation mechanisms that use potential energy storage elements, such as springs or additional masses for counterbalancing. These mechanisms aim to counteract the gravitational force on the linkage and reduce the payload impact. To achieve this, the spring or counterbalance mass is connected to a specific point on each linkage to reduce or eliminate the overall effect of gravitational force [1], [2].

Wongratnaphisan and Chew have found that a specific relative motion between the proximal and distal links is necessary to create a multi-DOF passive gravity compensator [3]. They proposed a parallelogram mechanism to achieve this motion. Kim and Song suggested a three-DOF passive gravity compensator that uses timing belts to create a parallelogram mechanism fulfilling the required relative motion condition [4]. However, using timing belts and cables instead of a parallelogram mechanism offers some advantages, such as reducing the robot's weight and complexity. Consequently, this approach has been widely researched [5], [6], [7], [8].

The associate editor coordinating the review of this manuscript and approving it for publication was Tao Liu.

Also, Cho et al. proposed a gravity compensator for a manipulator arm with a hemispherical workspace [9] using three bevel gears to create relative motion between links one and two. This design approach has been applied in other studies as well [10], [11], [12]. Cui et al. proposed a similar two-DOF system to achieve relative motion between proximal and distal links but used noncircular discs instead of bevel gears [13].

Numerous studies have utilized a cam shape to create torques for gravity compensation mechanisms. For instance, Ulrich and Kumar proposed a two-DOF gravity compensator that applies a cam-follower mechanism with a tension spring [14]. They designed a cam shape to compensate for the mass of each link, and the spring was connected to a wire wrapped around each cam to create gravity compensation. Similarly, Koser proposed a cam-follower gravity compensator for two-DOF systems that employed compression springs instead of tension springs [15]. Lee et al. used a similar mechanism to produce a compact and modular one-DOF gravity compensator [16]. Also, Takesue et al. also utilized the cam-follower mechanism to create a variable gravity compensation system [17], where they regulated the load that this gravity compensation system could manage by turning a knob. Others have applied this mechanism in various applications [18], [19], [20], [21].

Other unconventional compensators have also been proposed, such as that proposed by Boisclair et al. They used Halbach arrays as a one-DOF system gravity compensator [22]. Cheng et al. proposed a two-DOF system using an unconventional torsional compliance beam rather than a spring [23], whereas Trease and Dede suggested a similar compliance joint method, but using a torsion bar rather than a compliance beam [24]. Kuo and Wu [25] proposed a novel approach that employed a spring with a Cardan gear mechanism to achieve a compact gravity compensation mechanism.

Many researchers have proposed gravity compensator designs for specific fields. Woo et al. designed a hybrid gravity compensator system that used a counterweight and a spring together [26]. The system adjusted the compensation load by moving the counterweight position. Agrawal and Agrawal proposed a two-DOF gravity compensator system [27] for a leg orthosis, and Zhou et al. proposed a two-DOF gravity compensator system for a passive lower-limb exoskeleton for walking assistance [28]. The authors also used an optimization algorithm to optimize the design of a gravity compensator. This demonstrates the extensive potential applications of gravity compensation across various fields, including industrial robotics, medical technology, humanoid robotics, haptic devices, and exoskeleton designs [29], [30], [31], [32], [33], [34], [35].

Several studies have also focused on reducing the number of passive energy storage or partial compensation to minimize the complexity of the calculation and design. For instance, Kuo et al. proposed a gravity compensator in a reconfigurable mechanism [36], proving that a single spring can compensate for the gravitational force in two one-DOF reconfigurable systems. Maaroof et al. used Particle Swarm Optimization to compute the spring properties for a remote center-of-motion (RCM) mechanism [37], aiming to minimize the summation of actuator torques.

TABLE 1. Summary of gravity compensator research.

Ref /Year	Type	DOF	# energy elements	Goal
[29]/2019	Potential	3	2	Total
[31]/2020	Potential	2	1	Total
[6]/2021	Kinetic	4	4	Total
[30]/2021	Potential	2	1	Partial
[41]/2021	Potential	1	1	Total
[32]/2022	Hybrid	2	2	Total
[34]/2022	Kinetic	1	2	Partial
[35]/2022	Potential	2	2	Total
[38]/2022	Potential	2	2	Partial
[42]/2022	Kinetic	1	1	Total
[25]/2023	Potential	1	1	Total
[33]/2023	Hybrid	3	3	Total

Researchers have paid significant attention to optimization and partial gravity compensation methodologies in recent years, owing to the reduced complexity of the resulting mechanisms [31], [38], [39]. In our view, these strategies particularly appeal to industrial applications where cost-effectiveness is critical.

Over time, the trends in gravity compensation have progressed towards the creation of gravity compensators that can adjust to various loads. This means that passive gravity compensators can be adapted to handle different loads encountered by the manipulator arm. Adaptability is commonly achieved through mechanisms such as a changeable pivot lever or passive pulley system [40], [41], [42], [43].

To summarize, passive gravity compensators can be classified into three main categories:

1. Kinetic gravity compensators: This is the simplest method where a counterweight is used. However, it adds extra weight and inertia to the system.

2. Potential energy storage gravity compensators: This type of gravity compensator relies on the principle that the system is statically balanced if the total potential energy of the system remains constant for any configuration. Springs are the most commonly used potential energy-storage mechanism.

3. Combination of kinetic and potential energy storage or other types.

Most gravity compensators require the same number of compensating energy elements as the number of degrees of freedom (DOF). See Table 1. However, in some cases [29], the number of springs used is lower than the number of DOFs, and these mechanisms cannot be extended to higher DOFs. Some compensators aim for only partial compensation [31].

This research proposes a novel method for compensating gravity in n-degree-of-freedom mechanisms. Our approach uses a single potential energy element and a cam-follower mechanism to create spring displacement in the gravity compensator system. You can refer to Figure 1 that shows the

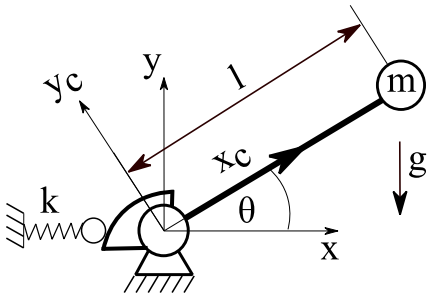

FIGURE 1. One DOF system's kinematic diagram.

one-link mechanism. For higher-DOF manipulators, we use parallelogram mechanisms to transmit all joint angles to the base. Each cam follower is placed next to the other in a series of connections. All displacements are summed, and only one spring compensates for all the joints. The details of this are described in the following sections.

II. ONE-DOF SYSTEM

To achieve static equilibrium, the potential energy of the entire system must remain constant [15]. In the model presented in this work, the sum of the potential energy from the spring and the potential energy from the linkage of the manipulator arm must remain constant in any configuration, as illustrated in Figure 1. The x-y coordinate was fixed to the ground at joint 1, and the X_c - Y_c coordinate was attached to the linkage.

We set $\theta = 90^{\circ}$ as the initial condition. The potential energy equation is given as

$$V_0 = \frac{1}{2}k\Delta x_0^2 + mgl\sin 90^{\circ} \tag{1}$$

where V_0 is the potential energy of the initial condition (a constant) and Δx_0 is the initial deformation (preload) of the spring. For any configuration, the potential energy can be calculated using

$$V_1(\theta) = \frac{1}{2}k\Delta x^2 + mgl\sin\theta \tag{2}$$

To maintain equilibrium, $V_1(\theta)$must equal to V_0, which gives us:

$$V_1(\theta) = V_0 \tag{3}$$

$$\therefore \Delta x(\theta) = \sqrt{(\Delta x_0^2 + \frac{2mgl}{k}(1-\sin\theta))} \tag{4}$$

For the system to be in equilibrium, the spring deformation $\Delta x(\theta)$ must follow Equation 4. By taking a set of these parameters ($\Delta x_0 = 5\ mm, m = 1.5\ kg, l = 0.1\ m, k = 1.5\ N/mm$.) Using the relation shown in Figure 2, the cam shape can be created.

III. MULTI-DOF SYSTEM

A. MULTI-DOF SOLUTION FOR THE SINGLE SPRING SYSTEM

In the previous section, Equation 4 was referenced. The general equation for a one-degree-of-freedom (DOF) gravity

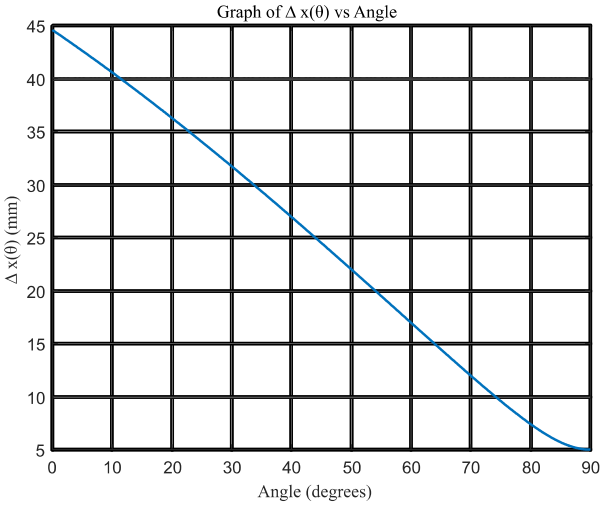

FIGURE 2. Relation between spring displacement vs joint angle.

compensator is expressed as follows:

$$\Delta x(\theta) = \sqrt{f(\theta)} \tag{5}$$

where $f(\theta)$ represents the mechanical parameters and configuration of the manipulator arm. In general, multiple potential energy elements can be used in a multi-DOF system to compensate for gravity. However, for higher-DOF manipulators, a single spring element is sufficient for gravity compensation. The general equation for gravity compensation can be written as:

$$\Delta x(\theta_1, \theta_2, \ldots \theta_n) = \sqrt{f(\theta_1, \theta_2, \ldots \theta_n)} \tag{6}$$

where [n] is the number of degrees of freedom of the manipulator arm. For a serial n-DOF manipulator, n cam followers are required (one for each joint). A complex n-dimensional cam follower can be used for a parallel n-DOF manipulator.

Consider n=2, then $\Delta x(\theta_1, \theta_2) = \sqrt{f(\theta_1, \theta_2)}$. In this case, the cam shape of the system can be a 3D complex shape, as shown in Figure 3.

The concept of expanding to higher DOF systems can be challenging in practice. To overcome this problem, we employed a square-root (SR) mechanism as a solution, as illustrated in Figure 4-5. The SR mechanism eliminated the square root from the RHS of Equation 6). In addition, parallelogram mechanisms were used to transfer the joint angles of each manipulator linkage. This enabled us to install cam-followers at the base, which were placed next to each other to form a series connection (cam series), as shown in Figure 6. The displacements from the cam followers were then summed, and the total displacement was transmitted to the SR mechanism. Finally, the output from the SR mechanism was directed to a linear compression spring.

B. SQUARE ROOT (SR) MECHANISM

The SR mechanism is a component of equation (6) and involves the square root term. It consists of an L-shaped

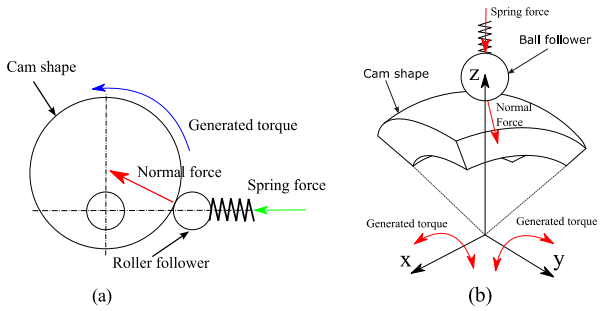

FIGURE 3. Kinematic diagram of Cam-follower: (a) a cam follower for 1 DOF system; (b) a complex cam follower for 2 DOF.

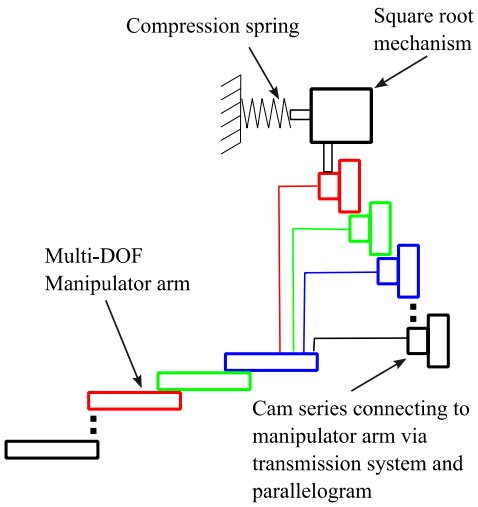

FIGURE 4. Diagram of a Multi-DOF system.

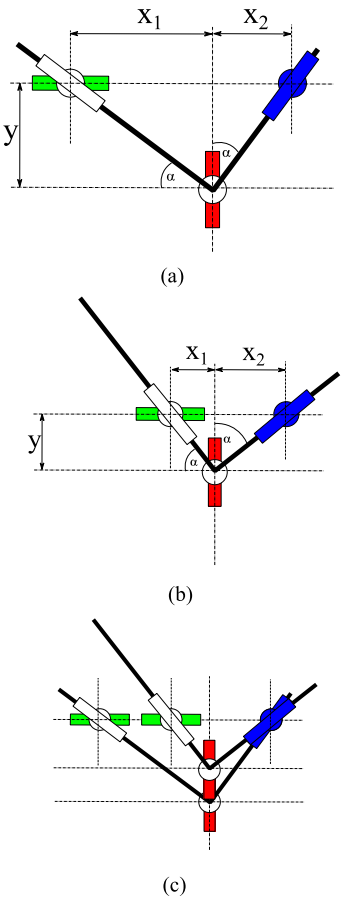

FIGURE 5. Square root (SR) mechanism: (a) Configuration 1; (b) Configuration 2; (c) Overlay image of configurations 1 and 2.

rigid-body assembly with a revolute and prismatic joint, as illustrated in Figure 5. The equation for the SR mechanism is expressed as

$$\tan\alpha = \frac{y}{x_1} = \frac{x_2}{y}$$
$$y = \sqrt{x_1 \cdot x_2} \tag{7}$$

where y and x_1 are the input and output variables, respectively, and x_2 is a predetermined fixed value used to adjust system size.

C. CAM SERIES

Figure 6 shows the cam-follower mechanism used in the multi-DOF manipulator. As the joint of the manipulator arm rotated, the cam rotated at the same angle, owing to the parallelogram. The cams were assembled in series and were in contact with each other through the follower. This implied that when one of the cams rotated, the overall displacement of the system changed. To represent the summation in the equation, we used cam-followers assembled in series.

D. POTENTIAL ENERGY OF A MULTI-DOF SYSTEM

Consider a multi-DOF manipulator, as shown in Figure 7. The manipulator was equipped with single-spring gravity compensation, as described above. The initial conditions were

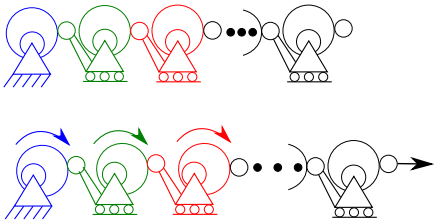

FIGURE 6. Cam series.

as follows: $\theta_1 = 90^\circ, \theta_2 = 0^\circ, \ldots, \theta_i = 0^\circ$. The potential energy equation for the n-DOF system can be expressed as follows:

$$V_1 = \frac{1}{2}k\Delta x_0^2 + m_1 g l_1 + m_2 g\,(D_1 + l_2) + \ldots + m_n g\,(D_1 + \ldots + D_{n-1} + l_n) \tag{8}$$

$$V_2 = \frac{1}{2}k\Delta x\,(\theta 1, \theta 2, \ldots, \theta i)^2 + m_1 g l_1 S1 + m_2 g\,(D_1 S1 + l_2 S12) + \ldots + m_n g\,(D_1 S1 + \ldots + D_{n-1} S12 \ldots i{-}1 + l_n S12 \ldots n) \tag{9}$$

where n is the number of DOF, V_1 is the potential energy at the initial conditions, and V_2 is the potential energy for any

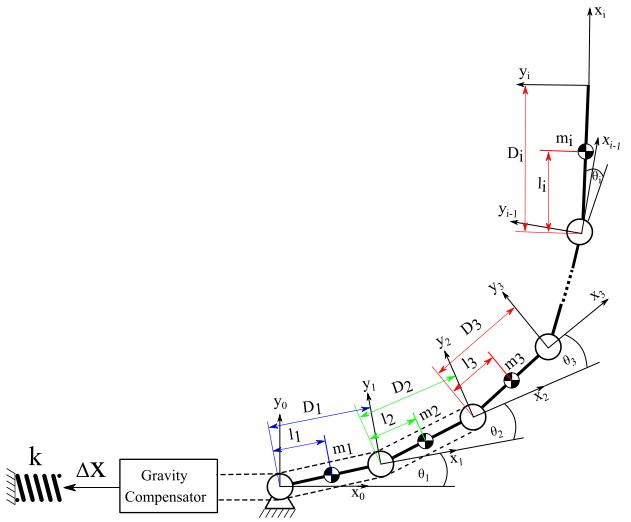

FIGURE 7. Multi DOF manipulator with a single spring gravity compensator system.

configuration. The equilibrium condition requires V_1 to be equal to V_2. For a system with a single spring and gravity compensator, the equation is

$$\begin{aligned}
&\frac{1}{2}k\Delta x(\theta 1, \theta 2, \ldots, \theta i)^2 \\
&= \frac{1}{2}k\Delta x_0^2 + m_1 g l_1 + m_2 g\,(D_1 + l_2) + \cdots \\
&\quad + m_l g\,(D_1 + \ldots + D_{i-1} + l_i) \\
&\quad - (m_1 g l_1 S1 + m_2 g\,(D_1 S1 + l_2 S12) + \ldots \\
&\quad + m_l g\,(D_1 S1 + \ldots + D_{i-1} S12 \ldots i - 1 + l_1 S12 \ldots i)) \\
&\frac{1}{2}k\Delta x(\theta 1, \theta 2, \ldots, \theta i)^2 \\
&= L - A_1 S1 - A_2 S12 - \cdots - A_n S12 \ldots i
\end{aligned}$$

Let's $L = \frac{1}{2}k\Delta x_0{}^2 + m_1 g l_1 + m_2 g\,(D_1 + l_2) + \cdots + m_i g\,(D_1 + \cdots D_{i-1} + l_i)$

$$\begin{aligned}
&A_n \\
&= g\left(m_n l_n + \sum_{m=n+1}^{i} m_m D_n\right) \quad : \text{i} = \text{DOF of system} \\
&\Delta x(\theta 1, \theta 2, \ldots, \theta i) \\
&= \sqrt{\frac{2}{k}\left(L - \sum_{n=1}^{i}\left(A_n \sin\left(\sum_{m=1}^{n}\theta_m\right)\right)\right)} \qquad (10)
\end{aligned}$$

where L and A_n are constant terms depending on the geometry of the manipulator arm.

IV. ONE AND THREE DOF PROTOTYPES

A. ONE DOF PROTOTYPE

We developed a basic 1 DOF prototype of a gravity compensator system to demonstrate its effectiveness. The prototype is illustrated in Figure 8. To test this, we conducted a static experiment and used a basic weight sensor to measure the force required to move the linkage from zero to 90 °, as shown in Figure 8. According to Table 2, the results showed a considerable decrease in the force required to move the linkage. It is worth noting that the sensor had a ±5 gram error margin.

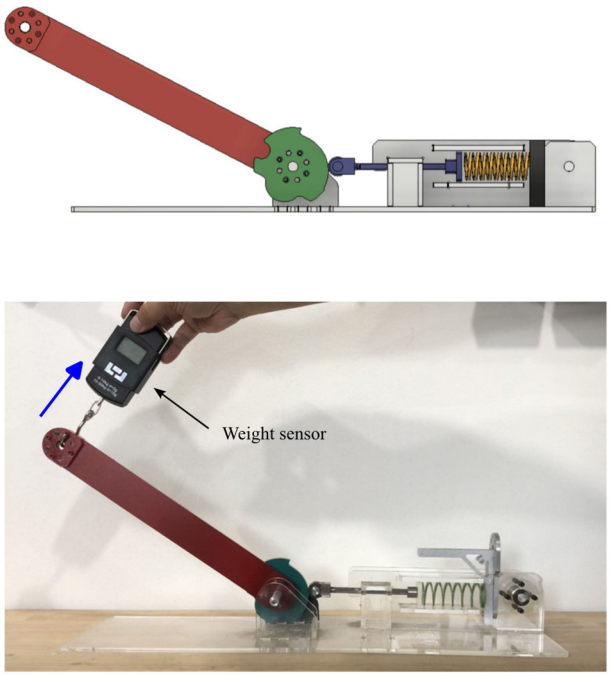

FIGURE 8. 1 DOF gravity compensator prototype.

TABLE 2. DOF experiment result.

Linkage Angle	No Compensator	With Compensator
Degrees	Pulling Force (Grams)	Pulling Force (Grams)
0	70	0
45	55	0
90	0	0

B. THREE DOF PROTOTYPE

We tested a one-degree-of-freedom prototype and then designed a sturdy three-degree-of-freedom serial-link prototype, as shown in Figure 9. We aimed to create a prototype with a weight and structure similar to that of an industrial manipulator. To ensure the strength of the structure, we made the linkages and structures mainly from 7075 aluminum, whereas all joints were made from stainless steel. We manufactured all critical parts, such as the cam and the square root mechanism, with a tolerance of ± 0.02 mm to minimize the effect of manufacturer imperfections on the prototype. Parts not directly involved in the mechanism were made with a tolerance of plus or minus 0.05 mm. The manufacturer controlled the quality of all the parts to ensure that they were made within the design tolerance.

We implemented timing belt parallelograms to transmit joint displacements to the cam-shaped followers. The cam

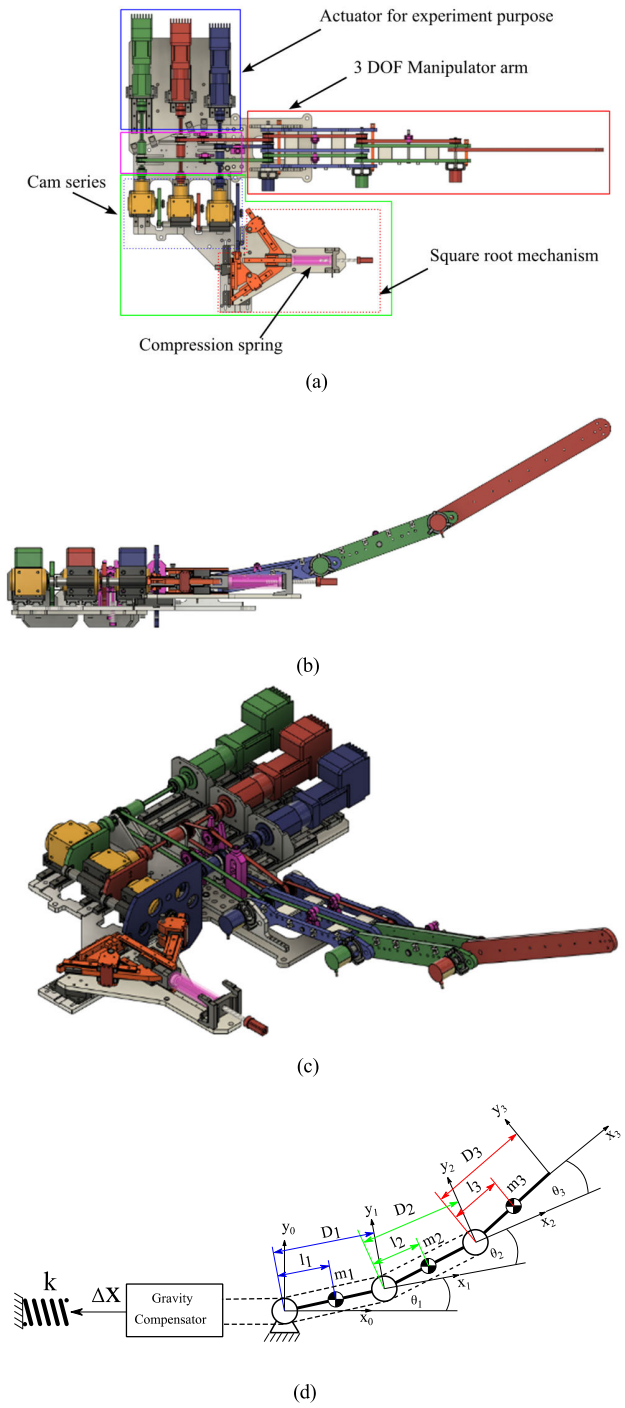

FIGURE 9. CAD model and the kinematic diagram of the 3 DOF Prototype. (a) Top view. (b) Side view. (c) 3D view. (d) Kinematic diagram.

shapes were made of S45C tool-grade steel to resist wear. All the cam-shaped followers were placed next to each other on a linear slide. We added follower displacements, and the total input displacement was fed into the SR mechanism. The output displacement from the SR mechanism was connected to a linear spring. The spring generated a gravity-compensating force through the SQ mechanism to cam followers for cable parallelogram transmissions and

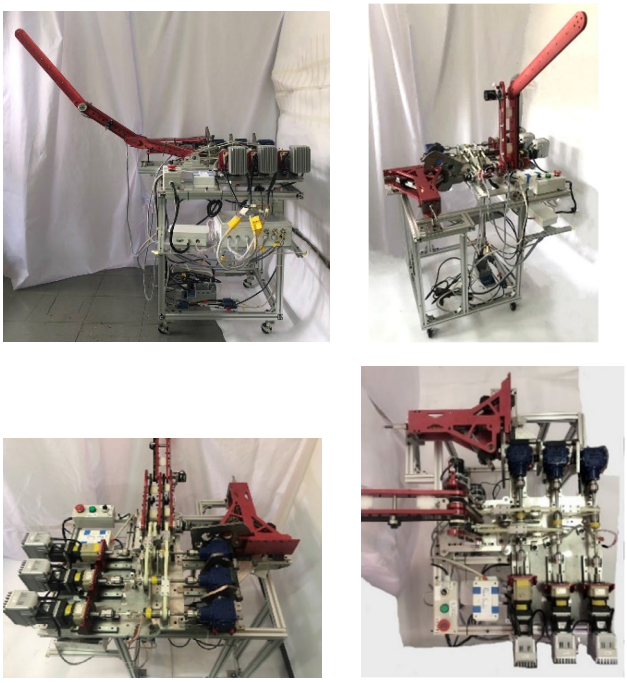

FIGURE 10. Pictures of the 3 DOF prototype.

FIGURE 11. Close-up picture of the mechanism. (a) Cam series. (b) Square root mechanism.

became anti-gravity torques for each joint. The complete prototype is illustrated in Figure 10.

We arranged the cam series side by side and connected them directly to the motors using spline shafts. This arrangement allowed the cam series to move along with the motor while rotating. The motors were installed for experimental purposes. The manipulator could passively remain in any configuration. Figure 11 shows a close-up picture of the Cam series and the square-root mechanism, with (a) representing the Cam series and (b) the square-root mechanism.

Referring to the diagram in Fig 9 and using equation (10), we can write the equation for the gravity compensator of the three DOF manipulator as follows $\Delta x\,(\theta 1,\theta 2,\theta 3)$, shown at the bottom of the next page:

Using equation 10 we can get the term below.

$$L = \frac{1}{2}k\Delta x_0^2 + m_1 g l_1 + m_2 g\,(D_1 + l_2) + m_3 g\,(D_1 + D_2 + l_3)$$

$$A_1 = m_1 g l_1 + m_2 g D_1 + m_3 g D_1$$

TABLE 3. Parameters of the prototype.

Linkage Number	m Kg	l mm	D mm
1	1.877	153.9	300
2	1.434	159.4	300
3	0.768	195.4	400

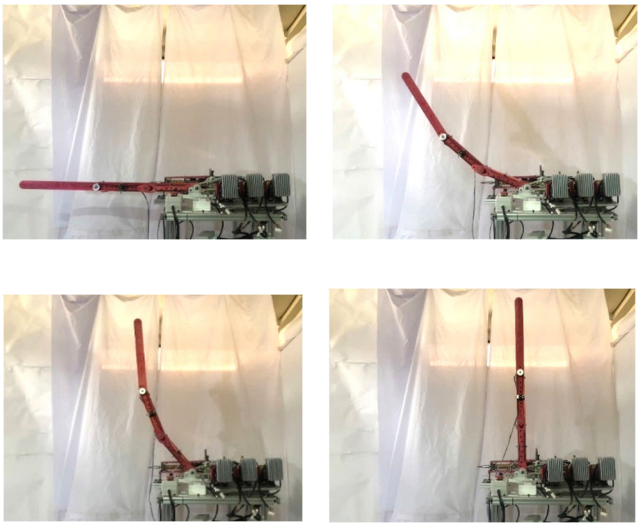

FIGURE 12. With gravity compensation, the manipulator can hold its position passively.

$$A_2 = m_2 g l_2 + m_3 g D_2$$
$$A_3 = m_3 g l_3$$

Thus,

$$\Delta x\,(\theta 1, \theta 2, \theta 3) = \sqrt{\frac{2}{k}\,(L - A_1 S1 - A_2 S12 - A_3 S123)} \tag{11}$$

L, A_1, A_2, and A_3 are constant terms that depend on the geometry of the arm of the manipulator. $S1 = \sin(\theta_1)$, $S12 = \sin(\theta_1 + \theta_2)$ and $S123 = \sin(\theta_1 + \theta_2 + \theta_3)$. The weight parameters for all three links were measured from the manufactured parts before they were inputted into the equation. The parameters of this prototype are listed in Table 3.

V. EXPERIMENT

The prototype had two modes of operation: passive and active. In passive mode, no motors were connected. With gravity compensation, the arm could easily move and maintain its position throughout all ranges of motion, as shown in Figure 12. You can watch a video of the experiment by clicking on the following link: https://www.youtube.com/watch?v=PED28ChCJXY.

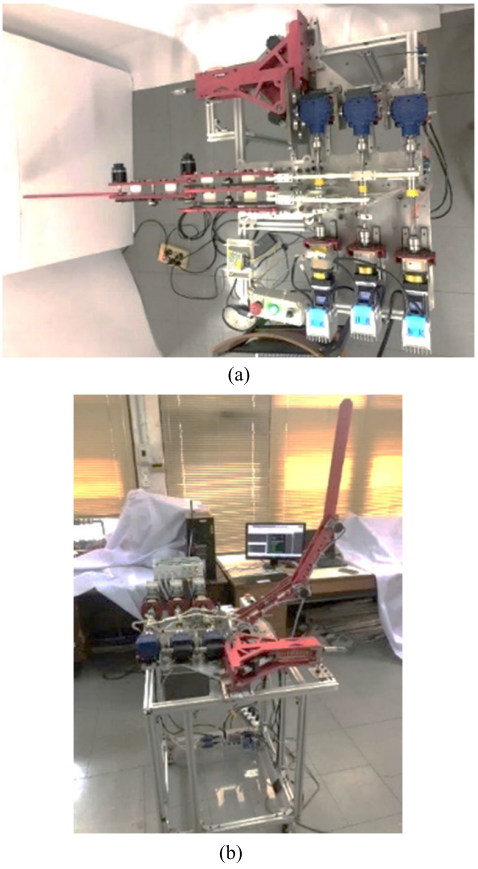

FIGURE 13. Experiment setup: (a) Top view; (b) DAQ and controller setup.

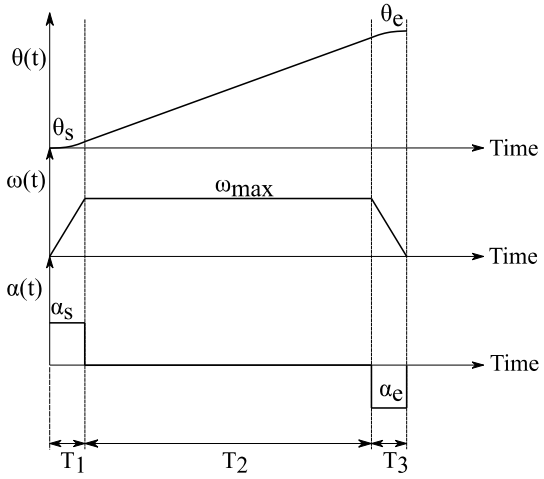

FIGURE 14. Experiment velocity profile.

The objective of this section is to verify the effectiveness of the single-spring gravity compensator on a manipulator arm with multiple degrees of freedom. We aimed to measure the torques required to move each linkage with and without the

$$\Delta x\,(\theta 1, \theta 2, \theta 3) = \sqrt{\begin{array}{c}\frac{2}{k}(\frac{1}{2}k\Delta x_0^2 + m_1 g l_1 + m_2 g\,(D_1 + l_2) + m_3 g\,(D_1 + D_2 + l_3) \\ - (m_1 g l_1 S1 + m_2 g\,(D_1 S1 + l_2 S12) + m_3 g\,(D_1 S1 + D_2 S12 + l_3 S123)))\end{array}}$$

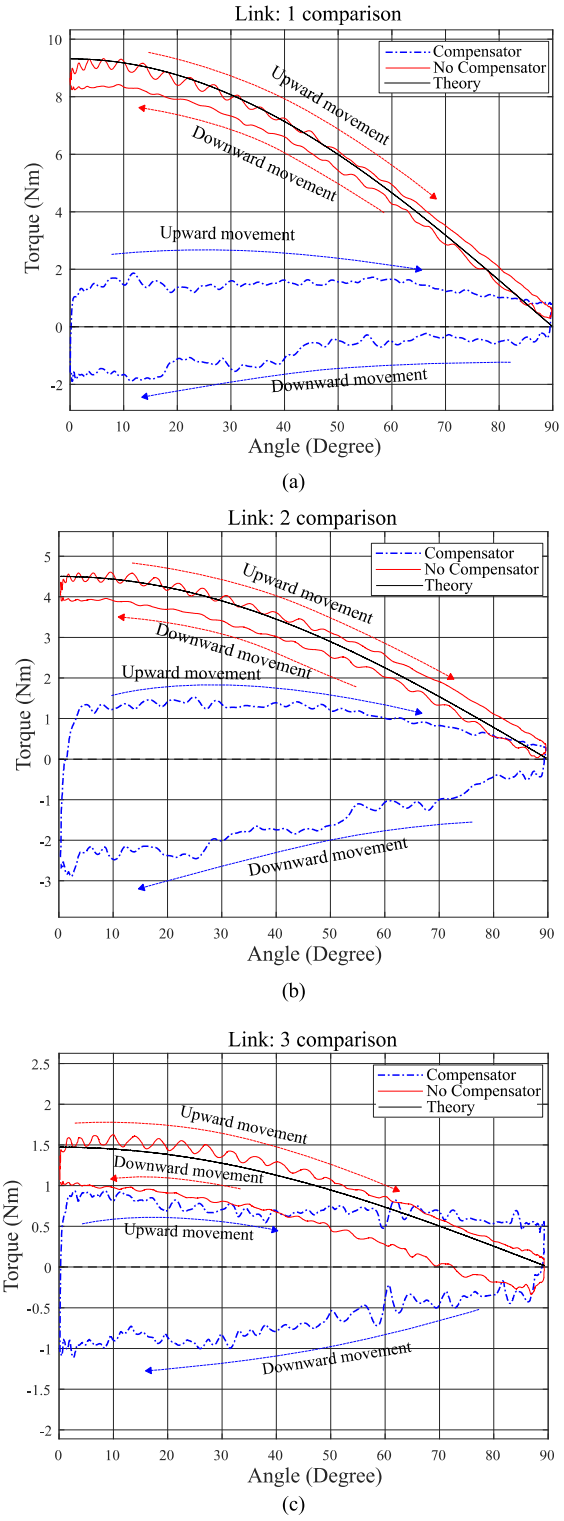

FIGURE 15. Comparisons of actual torques with and without gravity compensator. (a) Link 1; (b) Link 2; (c) Link 3.

gravity compensator. We decided to use the active mode of the manipulator, in which all motors were connected and controlled by the controllers. Two experiments were conducted to test and evaluate the gravity compensator.

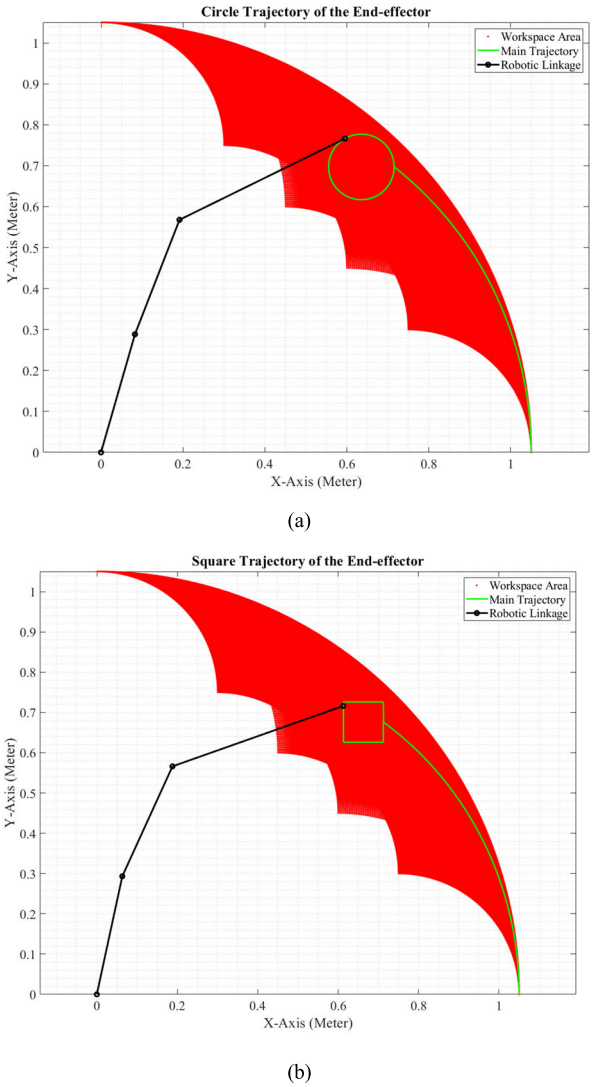

FIGURE 16. Reachable workspace with (a) circle path and (b) square path.

In the first experiment, we tested the prototype by commanding the motors to move all the linkages, covering a range of motions from 0 to 90 and back to 0 °. In the second experiment, we controlled the manipulator to follow the circular and square paths. Each experiment consisted of two rounds of repeated motion. The first round was performed without a gravity compensator, whereas the second round was performed with a gravity compensator.

A. EXPERIMENTAL SETUP

We used smart servomotors to control the movement of the linkages in our experimental setup. Each smart motor was connected to a planetary gearbox and spline shaft that extended from the cam series. To measure the torque at each joint, we used a biaxial strain gauge mounted on the shaft between the motor and the linkage. We calibrated the strain gauge using the ATI Gamma Force/Torque Sensor. Furthermore, a rotary encoder was installed at each joint to measure

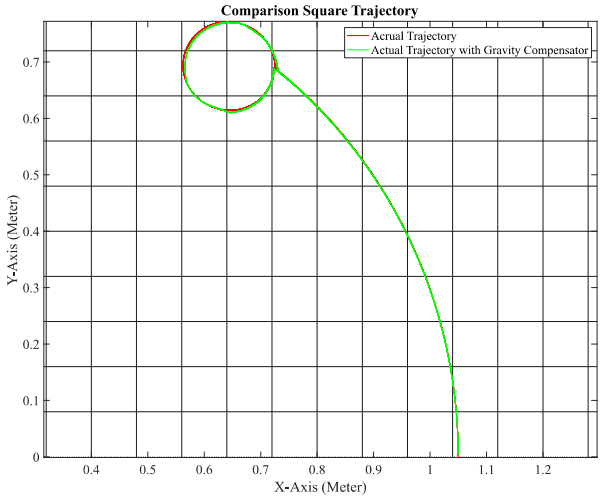

FIGURE 17. Circular trajectory: Actual trajectories with and without gravity compensator.

the joint angle. We gathered data from the strain gauge using the N.I. DAQ 9184. Sensoray 826 was responsible for motor control and data acquisition. Figure 13 shows actual images of the experimental setup.

B. EXPERIMENTAL RESULTS

1) RANGE OF MOTION EXPERIMENT

We conducted an experiment by moving all linkages from 0° to 90°, and then continuously brought them back to 0°. Figure 14 shows the velocity profiles for each linkage.

The experimental results are shown in Figure 15. The graphs show the driven torques versus the joint angles. The dashed and solid lines represent the torques with and without a gravity compensator, respectively. We could observe that the gravity compensator reduced the torques required for all the links. For linkage 1, the gravity compensator could reduce the motor torque by up to 77%, whereas the effects were smaller for links are smaller for links 2 and 3. This was because the gravity compensator exerted a force through all cam shapes using the same spring, resulting in a similar friction torque on each connecting linkage.

2) TRAJECTORY EXPERIMENT

In Figure 16, two paths were planned for the circular and square trajectories. The shaded area in the image represents a reachable workspace of the manipulator. To perform the trajectory paths, we started from the home position, moved to the starting position, completed the trajectory path, and then returned to the home position. We conducted experiments on both paths and found that the results were similar. In this description, we only discuss the results for the circular path. Figure 17 shows an overlay of the actual trajectories with and without gravity compensation. The trajectories were fairly close to each other.

Graphs (a), (b), and (c) in Figure 18 show the driven torques versus the joint angle for each link. The plots compare the

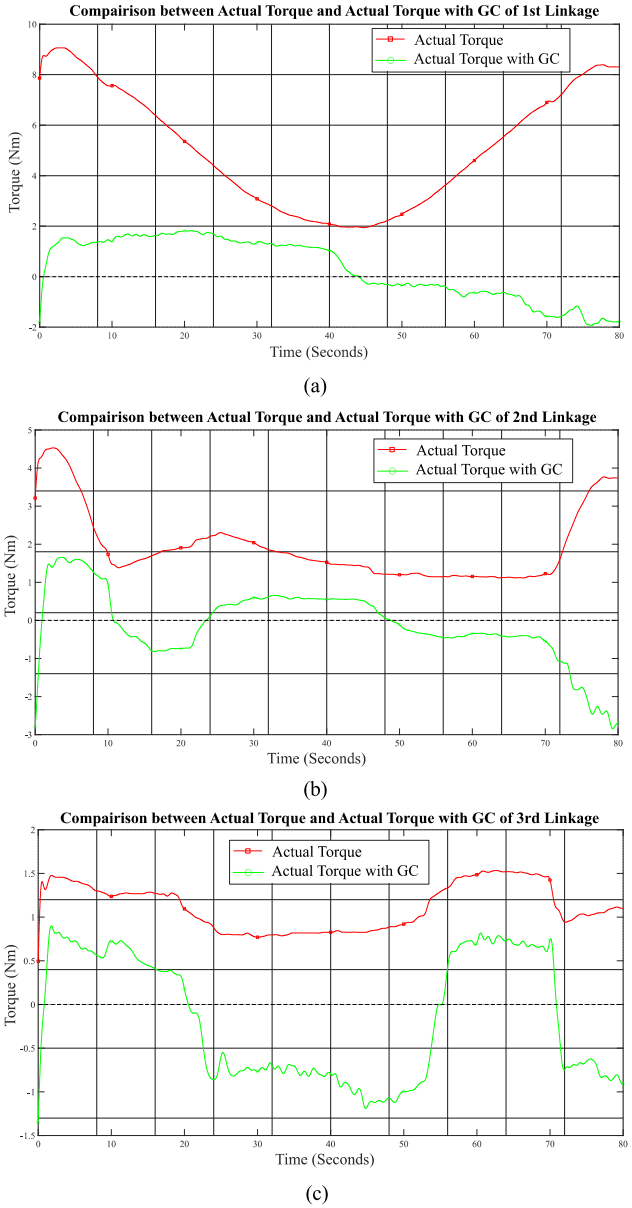

FIGURE 18. Comparisons of actual torques with and without gravity compensator. (a) Link 1; (b) Link 2; (c) Link 3.

actual driving torques with and without the gravity compensator. It was evident that the gravity compensator reduced the torques required for all the links.

Based on the obtained results, it was found that the average torques of links 1 to 3 were 5.10 Nm, 1.94 Nm, and 1.12 Nm without the gravity compensator. However, when the gravity compensator was used, the average torques decreased significantly to 1.12 Nm, 0.74 Nm, and 0.59 Nm, respectively.

Figure 19 shows the total power and energy utilized to operate the manipulator with and without the gravity compensator. The energy consumption was 29.05 J when the gravity compensator was not used, whereas implementing gravity compensation resulted in a significant decrease in energy consumption, with a total energy usage of 9.35 J.

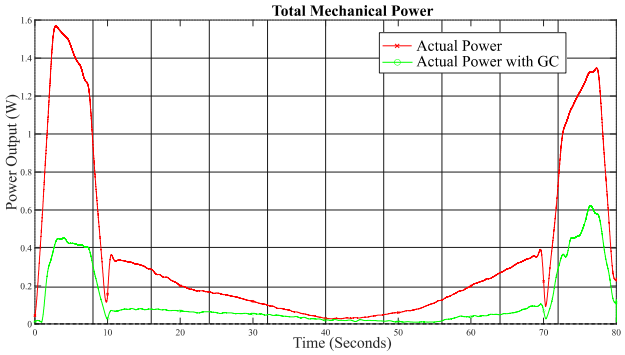

(a)

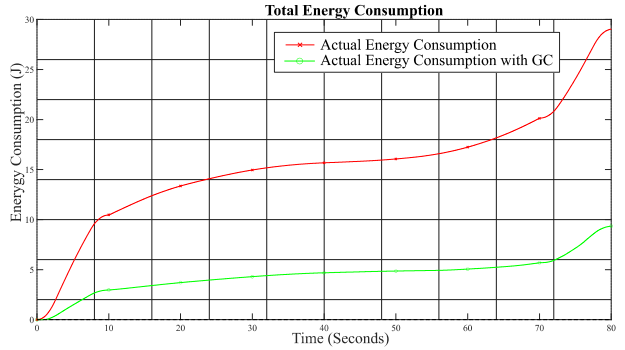

(b)

FIGURE 19. Comparisons of actual power (a) and energy (b) with and without gravity compensator.

VI. CONCLUSION AND FUTURE WORK

We developed an innovative gravity compensation system that can be utilized for multi-DOF manipulator systems with only one linear spring. To test its effectiveness, we constructed a sturdy three-DOF manipulator testbed and conducted experiments. The results were impressive, as the gravity compensator significantly reduced the torques, power, and energy consumption required for the entire system. On average, the torques were reduced by up to 78%, while the total energy consumption was reduced by up to 68%. This passive gravity compensator not only made manipulators safer by requiring less power but also served as an excellent option for power-efficient robotic manipulator designs.

However, our experiments revealed some primary errors arising from mechanical friction, spline shaft stiffness, and tolerance of the compression spring. The friction in this system had a similar effect on all connecting joints. This could be improved by providing more rigid mechanisms and structures. Additionally, we are planning to introduce an adjustable mechanism to compensate for the payload of the manipulator.

ACKNOWLEDGMENT

The authors thank Parvares Sretacha for providing the experimental equipment.

During the preparation of this work, they used ChatGPT and Paperpal Preflight to check the grammar and improve readability. After using this tool/service, they reviewed and edited the content as needed and took full responsibility for the content of the publication.

REFERENCES

[1] V. Arakelian, "Gravity compensation in robotics," *Adv. Robot.*, vol. 30, no. 2, pp. 79–96, Jan. 2016.

[2] Y. R. Chheta, R. M. Joshi, K. K. Gotewal, and M. ManoahStephen, "A review on passive gravity compensation," in *Proc. Int. Conf. Electron., Commun. Aerosp. Technol. (ICECA)*, vol. 1, Apr. 2017, pp. 184–189.

[3] T. Wongratanaphisan and M. Chew, "Gravity compensation of spatial two-DOF serial manipulators," *J. Robotic Syst.*, vol. 19, no. 7, pp. 329–347, Jul. 2002.

[4] H.-S. Kim and J.-B. Song, "Low-cost robot arm with 3-DOF counterbalance mechanism," in *Proc. IEEE Int. Conf. Robot. Autom.*, Karlsruhe, Germany, May 2013, pp. 4183–4188.

[5] H.-S. Kim and J.-B. Song, "Multi-DOF counterbalance mechanism for a service robot arm," *IEEE/ASME Trans. Mechatronics*, vol. 19, no. 6, pp. 1756–1763, Dec. 2014.

[6] H. Jamshidifar, A. Khajepour, T. Sun, N. Schmitz, S. Jalali, R. Topor-Gosman, and J. Dong, "A novel mechanism for gravity-balancing of serial robots with high-dexterity applications," *IEEE Trans. Med. Robot. Bionics*, vol. 3, no. 3, pp. 750–761, Aug. 2021.

[7] D. Lee and T. Seo, "Lightweight multi-DOF manipulator with wire-driven gravity compensation mechanism," *IEEE/ASME Trans. Mechatronics*, vol. 22, no. 3, pp. 1308–1314, Jun. 2017.

[8] Y. Peng and W. Bu, "Design of gravity-balanced exoskeletons with linkage-belt hybrid transmissions," *Mechanism Mach. Theory*, vol. 170, Apr. 2022, Art. no. 104660.

[9] C. Cho, W. Lee, and S. Kang, "Static balancing of a manipulator with hemispherical work space," in *Proc. IEEE/ASME Int. Conf. Adv. Intell. Mechatronics*, Montréal, QC, Canada, Jul. 2010, pp. 1271–1272.

[10] C. Cho and S. Kang, "Design of a static balancing mechanism for a serial manipulator with an unconstrained joint space using one-DOF gravity compensators," *IEEE Trans. Robot.*, vol. 30, no. 2, pp. 421–431, Apr. 2014.

[11] C. Cho and S. Kang, "Design of a static balancing mechanism with unit gravity compensators," in *Proc. IEEE/RSJ Int. Conf. Intell. Robots Syst.*, Sep. 2011, pp. 1857–1862.

[12] S.-H. Kim and C.-H. Cho, "Static balancer of a 4-DOF manipulator with multi-DOF gravity compensators," *J. Mech. Sci. Technol.*, vol. 31, no. 10, pp. 4875–4885, Oct. 2017.

[13] M. C. Cui, S. X. Wang, and J. M. Li, "Spring gravity compensation using the noncircular pulley and cable for the less-spring design," in *Proc. 14th IFToMM World Congr.*, Taipei, Taiwan, 2015, pp. 2–4.

[14] N. Ulrich and V. Kumar, "Passive mechanical gravity compensation for robot manipulators," in *Proc. IEEE Int. Conf. Robot. Autom.*, Sacramento, CA, USA, Jan. 1991, pp. 1536–1537.

[15] K. Koser, "A cam mechanism for gravity-balancing," *Mech. Res. Commun.*, vol. 36, no. 4, pp. 523–530, Jun. 2009.

[16] G. Lee, D. Lee, and Y. Oh, "One-piece gravity compensation mechanism using cam mechanism and compression spring," *Int. J. Precis. Eng. Manuf.-Green Technol.*, vol. 5, no. 3, pp. 415–420, Jul. 2018.

[17] N. Takesue, T. Ikematsu, H. Murayama, and H. Fujimoto, "Design and prototype of variable gravity compensation mechanism (VGCM)," *J. Robot. Mechatronics*, vol. 23, no. 2, pp. 249–257, Apr. 2011.

[18] J. Seok, S. Kang, and W. Lee, "Design of variable release torque-based compliant spring-clutch and torque estimation," in *Proc. IEEE/RSJ Int. Conf. Intell. Robots Syst.*, Chicago, IL, USA, Sep. 2014, pp. 2873–2878.

[19] K. O. Lund, "Means and method to counterbalance the weight of body," U.S. Patent 4 768 762, Sep. 6, 1988.

[20] M. Asgari, P. T. Hall, B. S. Moore, and D. L. Crouch, "Wearable shoulder exoskeleton with spring-cam mechanism for customizable, nonlinear gravity compensation," in *Proc. 42nd Annu. Int. Conf. IEEE Eng. Med. Biol. Soc. (EMBC)*, Jul. 2020, pp. 4926–4929.

[21] J. Hull, R. Turner, and A. T. Asbeck, "Design and preliminary evaluation of two tool support arm exoskeletons with gravity compensation," *Mechanism Mach. Theory*, vol. 172, Jun. 2022, Art. no. 104802.

[22] J. Boisclair, P.-L. Richard, T. Laliberté, and C. Gosselin, "Gravity compensation of robotic manipulators using cylindrical Halbach arrays," *IEEE/ASME Trans. Mechatronics*, vol. 22, no. 1, pp. 457–464, Feb. 2017.

[23] Z. Cheng, S. Foong, D. Sun, and U.-X. Tan, "Towards a multi-DOF passive balancing mechanism for upper limbs," in *Proc. IEEE Int. Conf. Rehabil. Robot. (ICORR)*, Aug. 2015, pp. 508–513.

[24] B. Trease and E. Dede, "Statically-balanced compliant four-bar mechanism for gravity compensation," in *Proc. ASME Student Mechanism Design Competition*, Ann Arbor, MI, USA, 2004, pp. 1–13.

[25] C.-H. Kuo and Y.-X. Wu, "Perfect static balancing using cardan-gear spring mechanisms," *Mechanism Mach. Theory*, vol. 181, Mar. 2023, Art. no. 105229.
[26] J. Woo, J.-T. Seo, and B.-Y. Yi, "A static balancing method for variable payloads by combination of a counterweight and spring and its application as a surgical platform," *Appl. Sci.*, vol. 9, no. 19, p. 3955, Sep. 2019.
[27] A. Agrawal and S. K. Agrawal, "Design of gravity balancing leg orthosis using non-zero free length springs," *Mechanism Mach. Theory*, vol. 40, no. 6, pp. 693–709, Jun. 2005.
[28] L. Zhou, W. Chen, W. Chen, S. Bai, J. Zhang, and J. Wang, "Design of a passive lower limb exoskeleton for walking assistance with gravity compensation," *Mechanism Mach. Theory*, vol. 150, Aug. 2020, Art. no. 103840.
[29] S.-H. Yun, J. Seo, J. Yoon, H. Song, Y.-S. Kim, and Y.-J. Kim, "3-DOF gravity compensation mechanism for robot waists with the variations of center of mass," in *Proc. IEEE/RSJ Int. Conf. Intell. Robots Syst. (IROS)*, Nov. 2019, pp. 3565–3570.
[30] J.-R. Li, J.-L. Fu, S.-C. Wu, and Q.-H. Wang, "An active and passive combined gravity compensation approach for a hybrid force feedback device," *Proc. Inst. Mech. Eng. C, J. Mech. Eng. Sci.*, vol. 235, no. 19, pp. 4368–4381, Oct. 2021.
[31] J. Reinecke, B. Deutschmann, A. Dietrich, and M. Hutter, "An anthropomorphic robust robotic torso for ventral/dorsal and lateral motion with weight compensation," *IEEE Robot. Autom. Lett.*, vol. 5, no. 3, pp. 3876–3883, Jul. 2020.
[32] L. Meng, S. Kang, and W. Chou, "Design and development of a novel haptic device with gravity compensation for teleoperation," in *Proc. IEEE Int. Conf. Mechatronics Autom. (ICMA)*, Aug. 2022, pp. 286–291.
[33] A. B. Aldanmaz, O. Ayit, G. Kiper, and M. Í. C. Dede, "Gravity compensation of a 2R1T mechanism with remote center of motion for minimally invasive transnasal surgery applications," *Robotica*, vol. 41, no. 3, pp. 807–820, Mar. 2023.
[34] L. Jin, X. Duan, R. He, F. Meng, and C. Li, "Improving the force display of haptic device based on gravity compensation for surgical robotics," *Machines*, vol. 10, no. 10, p. 903, Oct. 2022.
[35] J. Wang, Y. Kan, T. Zhang, Z. Zhang, and M. Xu, "Model analysis and experimental study of lower limb rehabilitation training device based on gravity balance," *Machines*, vol. 10, no. 7, p. 514, Jun. 2022.
[36] C.-H. Kuo, V. L. Nguyen, D. Robertson, L.-T. Chou, and J. L. Herder, "Statically balancing a reconfigurable mechanism by using one passive energy element only: A case study," *J. Mech. Robot.*, vol. 13, no. 4, pp. 2–3, Aug. 2021.
[37] O. W. Maaroof, S. Z. Saeed, and M. Í. C. Dede, "Partial gravity compensation of a surgical robot," *Int. J. Adv. Robotic Syst.*, vol. 18, no. 3, May 2021, Art. no. 172988142110154.
[38] V. L. Nguyen, "A design approach for gravity compensators using planar four-bar mechanisms and a linear spring," *Mechanism Mach. Theory*, vol. 172, Jun. 2022, Art. no. 104770.
[39] A. Alamdari, R. Haghighi, and V. Krovi, "Gravity-balancing of elastic articulated-cable leg-orthosis emulator," *Mechanism Mach. Theory*, vol. 131, pp. 351–370, Jan. 2019.
[40] J. Kim, J. Moon, J. Kim, and G. Lee, "Compact variable gravity compensation mechanism with a geometrically optimized lever for maximizing variable ratio of torque generation," *IEEE/ASME Trans. Mechatronics*, vol. 25, no. 4, pp. 2019–2026, Aug. 2020.
[41] D. Franchetti, G. Boschetti, and B. Lenzo, "Passive gravity balancing with a self-regulating mechanism for variable payload," *Machines*, vol. 9, no. 8, p. 145, Jul. 2021.
[42] R. Furnémont, T. Verstraten, D. Lefeber, and B. Vanderborght, "Prismatic gravity compensator for variable payloads," *IEEE Robot. Autom. Lett.*, vol. 7, no. 2, pp. 3749–3756, Apr. 2022.
[43] J. Kim, J. Moon, J. Ryu, S. Kim, J. Yoon, and G. Lee, "A novel energy-efficient actuator integrated with compact variable gravity compensation module," *Mechanism Mach. Theory*, vol. 177, Nov. 2022, Art. no. 105031.

KRITTANAI SAJJAPONGSE received the B.S. degree in mechanical engineering from Chulalongkorn University, Bangkok, Thailand, in 2008, and the M.S. degree in mechanical engineering from Nagoya Institute of Technology, Nagoya, Japan, in 2011. He is currently pursuing the Ph.D. degree in mechanical engineering with Chulalongkorn University.

In 2008, along with his team "Plasma RX," he won the World Championship Rescue Robot Competition, Suzhou, China. In the M.S. degree in Japan, he specialized in passive mechanisms and mechanical design. His research in Japan is "Assist Level Walking of Passive Biped Walker With Upper Body and Ankle Spring Mechanisms." From 2011 to 2015, he was with Aichi Steel, Nagoya, as a Hot Forging Die Design Engineer. He is also assisting in the development of the forging line with Aichi Forge Thailand.

WITAYA WANNASUPHOPRASIT received the bachelor's degree from the King Mongkut's Institute of Technology, Ladkrabang, Bangkok, Thailand, in 1990, and the M.S. and Ph.D. degrees from Northwestern University. He developed the world's first collaborative robot (Cobot). As the Co-Founder of Cobotics Inc., he further advanced industrial cobots and intelligent assist devices. He is currently an Associate Professor with Chulalongkorn University, Bangkok. He is also the Director of the International School of Engineering, Chulalongkorn University. His research interests include cobots, haptic interfaces, and human interaction with intelligent systems. He received the Best Paper Award from the IEEE International Conference on Robotics and Automation, in 1996, and the ASME International Mechanical Engineering Congress and Exposition (MHED Division), in 1998. From 2018 to 2022, he was the President of the Thai Robotics Society.